Science Signaling
AAAS

Supplementary Materials for

Cbl-b mitigates the responsiveness of naive CD8$^+$ T cells that experience extensive tonic T cell receptor signaling

Joel Eggert *et al.*

Corresponding author: Byron B. Au-Yeung, byron.au-yeung@emory.edu

Sci. Signal. **18**, eadh0439 (2024)
DOI: 10.1126/scisignal.adh0439

The PDF file includes:

Other Supplementary Material for this manuscript includes the following:

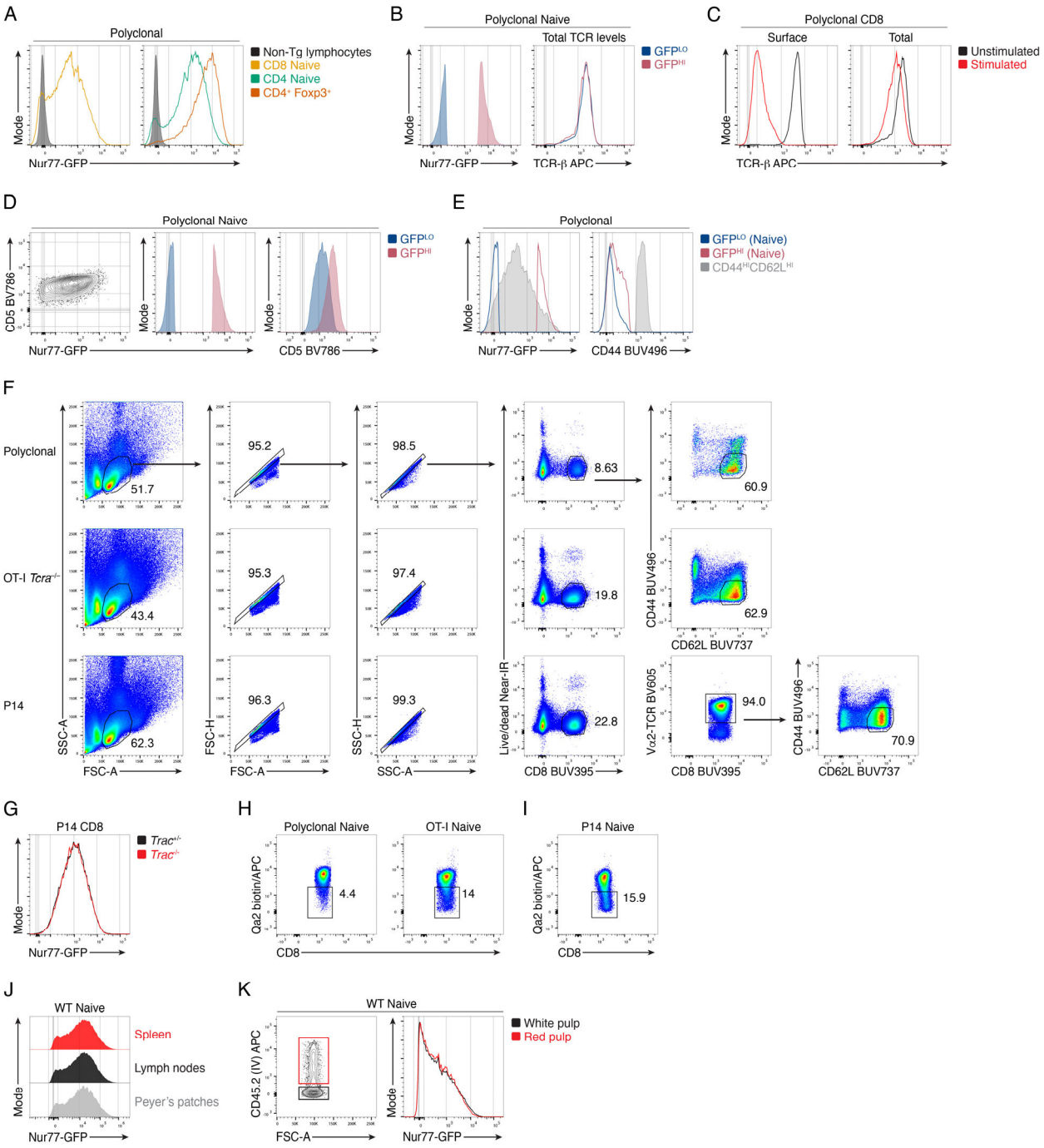

Fig. S1. Supporting data for the heterogeneity of tonic TCR signaling intensity in naive CD8$^+$ T cells. (**A**) Representative flow cytometry plots of Nur77-GFP fluorescence of naive, splenic, polyclonal CD44^{LO} CD62L^{HI} CD8$^+$ (left) and CD4$^+$ cells (cyan) or CD4$^+$ Foxp3-IRES-RFP$^+$ (red) T cells (right). Data represent two independent experiments with n = 7 mice. (**B**) Overlaid histogram (left) depicts Nur77-GFP fluorescence for naive GFP^{LO} and GFP^{HI} cells in the spleen. Histogram (right) shows the expression of TCR-β in permeabilized, naive GFP^{LO} and GFP^{HI} CD8$^+$ T cells. Data represent two independent experiments with n = 4 mice. (**C**) Histograms display the staining intensity of TCR-β at the surface (left) or total (right) level. Polyclonal CD8$^+$ T cells were either unstimulated (black) or stimulated for 90 minutes with 10 µg/ml anti-CD3 and 4 µg/ml anti-CD28 (red). Data represent two independent experiments with n = 4 mice. (**D**) Contour plot (left) shows CD5 and Nur77-GFP expression by total naive polyclonal CD8$^+$ T

cells. Overlaid histogram (center) depicts Nur77-GFP fluorescence for GFP^{LO} and GFP^{HI} cells. Histogram (right) shows CD5 expression in GFP^{LO} and GFP^{HI} populations. Data represent three independent experiments with n = 6 mice. (**E**) Histograms depict Nur77-GFP expression (left) and CD44 staining intensity (right) of polyclonal naive GFP^{LO} and GFP^{HI} cells or $CD44^{HI}$ $CD62L^{HI}$ cells. Data represent three independent experiments with n = 6 mice. (**F**) Representative gating of naive polyclonal, OT-I, and P14 $CD8^+$ T cells. Numbers indicate the percentage of cells within each gate. (**G**) Histogram shows Nur77-GFP expression in $Trac^{+/-}$ (black) and $Trac^{-/-}$ (red) P14 $CD8^+$ T cells. Data represent two independent experiments with n = 6 mice. (**H**) Representative dot plots depict Qa2 and CD8 expression in naive polyclonal or OT-I $CD8^+$ T cells in mice aged 6-9 weeks. Numbers indicate the percentage of cells within the indicated gates. Data represent two independent experiments with n = 4 mice. (**I**) Representative dot plots depict Qa2 and CD8 expression in naive P14 $CD8^+$ T cells in mice aged 6-13 weeks. Data represent two independent experiments with n = 3 mice. (**J**) Offset histograms show Nur77-GFP expression in naive TCR polyclonal $CD8^+$ T cells harvested from the spleen, mesenteric lymph nodes, or Peyer's Patches. Data represent two independent experiments with n = 3 mice. (**K**) Flow cytometry plots of naive polyclonal $CD8^+$ T cells after intravascular labeling of cells in the red pulp by intravenous injection of CD45.2-APC antibody intravenously prior to euthanasia. Data represent three independent experiments with n = 3 mice.

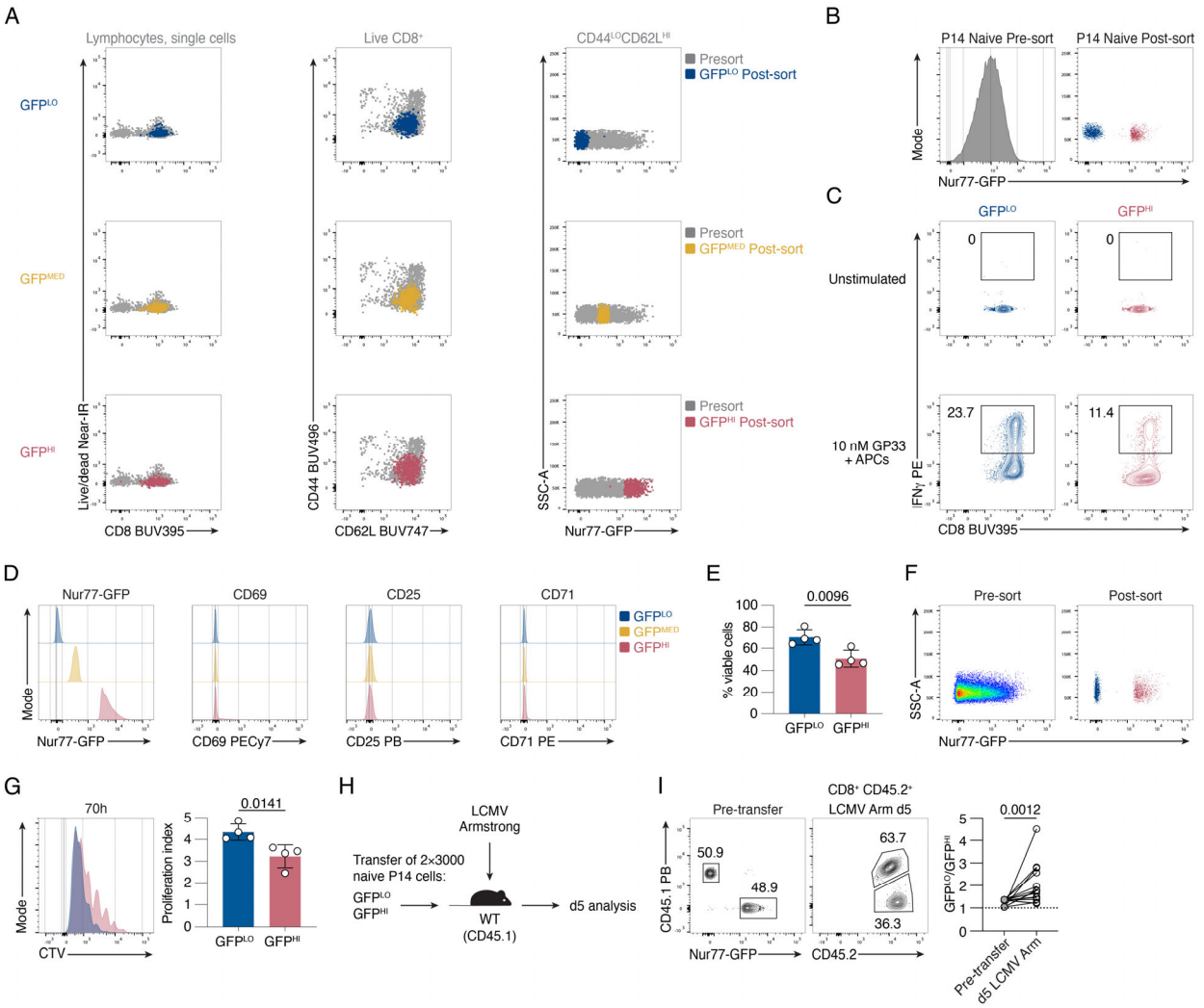

Fig. S2. Supporting data for the negative correlation between extensive tonic TCR signaling and naive, polyclonal CD8 T cell responsiveness. (**A**) Representative backgating analysis of sorted naive polyclonal GFP^{LO}, GFP^{MED}, and GFP^{HI} cells. Sorted cells were gated on lymphocytes and single cells, and the pre-sort sample was gated as indicated in grey above the plots. (**B**) Representative histogram (left) and dot plot (right) depict Nur77-GFP expression in total and sorted GFP^{LO} and GFP^{HI} naive P14 CD8^{+} T cells, respectively. Data represent two independent experiments with $n = 5$ mice. (**C**) Representative contour plots depict CD8 and IFNγ expression by unstimulated and stimulated viable P14 CD8^{+} T cells after a 45 min IFNγ secretion assay. Cells were stimulated for 16 hours with GP33 peptide and APCs before the secretion assay. Numbers indicate the percentage of cells within the indicated gates. Data represent two independent experiments with $n = 5$ mice. (**D**) Histograms show the expression of the indicated activation markers in unstimulated control cells. Data represent three independent experiments with $n = 6$ mice. (**E**) The frequency of viable CD8^{+} T cells was determined after 24 hours of stimulation with 0.25 µg/ml anti-CD3 and APCs. Data represent four independent experiments with $n = 4$ mice. (**F**) Representative flow cytometry plots of the pre-sort Nur77-GFP distribution (left) and sorted GFP^{LO} and GFP^{HI} naive, polyclonal CD8 T cell populations (right). Data represent four independent experiments with $n = 4$ mice. (**G**) CTV-labeled naive, polyclonal GFP^{LO} and GFP^{HI} CD8^{+} T cells were incubated for 70 hours with 0.25 µg/ml anti-CD3 and APCs. The representative flow cytometry plot was gated on viable CD8^{+} T cells. The graph depicts the proliferation index (the average number of divisions in cells that divided at least once). Data represent four independent experiments with $n = 4$ mice. (**H**) Schematic overview of the competitive-transfer experiment. 3000 cells each of GFP^{LO} and GFP^{HI} naive P14 cells were co-transferred into WT recipients, which were

then infected with LCMV Armstrong (2×10^5 PFU i.p.). (**I**) Contour plots (left) depict mixed GFP^{LO} and GFP^{HI} cells pre-transfer and (right) cells harvested from the spleen on day five post-infection gated on viable donor cells. Scatterplot displays the ratio of GFP^{LO} to GFP^{HI} P14 donor cells pooled from three independent experiments with 15 mice. Each symbol represents one mouse. In (E) and (G), bars depict means, error bars depict ± s.d., and each symbol represents one mouse. Statistical testing was performed by unpaired two-tailed Student's *t* test (E and G) or by two-tailed Wilcoxon matched-pairs signed-rank test (I).

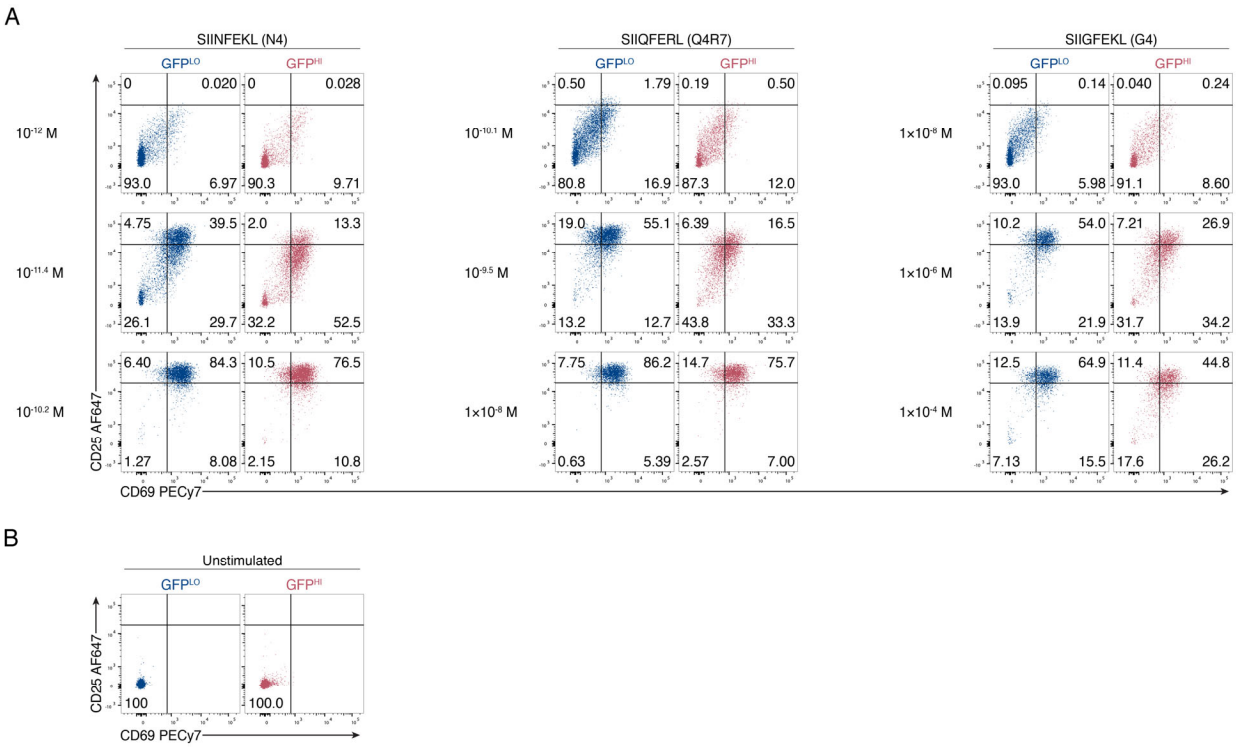

Fig. S3. Supporting data for the negative correlation between extensive tonic TCR signaling and naive OT-I cell responsiveness. (**A**) Representative flow cytometry plots depicting CD25 and CD69 expression after 16 hours of stimulation with indicated peptide concentrations are shown from one experiment. Panels in the first row represent suboptimal peptide concentrations. Panels in the second row depict peptide concentrations on the linear part of the dose-response curve. Panels in the third row show saturating peptide concentrations. Numbers indicate the percentage of cells within the indicated gates. (**B**) Plots show CD25 and CD69 expression in unstimulated GFP^{LO} and GFP^{HI} naive OT-I cells. Data in (A) and (B) represent three independent experiments with $n = 3$ biological replicates.

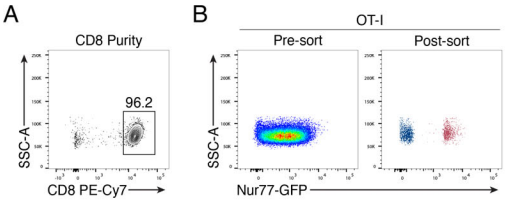

Fig. S4. Supporting data that GFP^{HI} CD8^{+} T cells exert less TCR-mediated tension forces and exhibit attenuated proximal and integrated TCR signaling. (**A**) CD8 staining of OT-I cells post-negative enrichment. The percentage of CD8-positive cells was >96% for all experiments. (**B**) Dot plots depict Nur77-GFP fluorescence intensity for total OT-I cells (left) and sorted GFP^{LO} and GFP^{HI} cells (right). CD8^{+} T cells were enriched by negative selection before sorting. Cells are gated on viable, CD4$^{–}$ CD19$^{–}$ cells. Data in (A) and (B) represent three independent experiments with n = 3 mice.

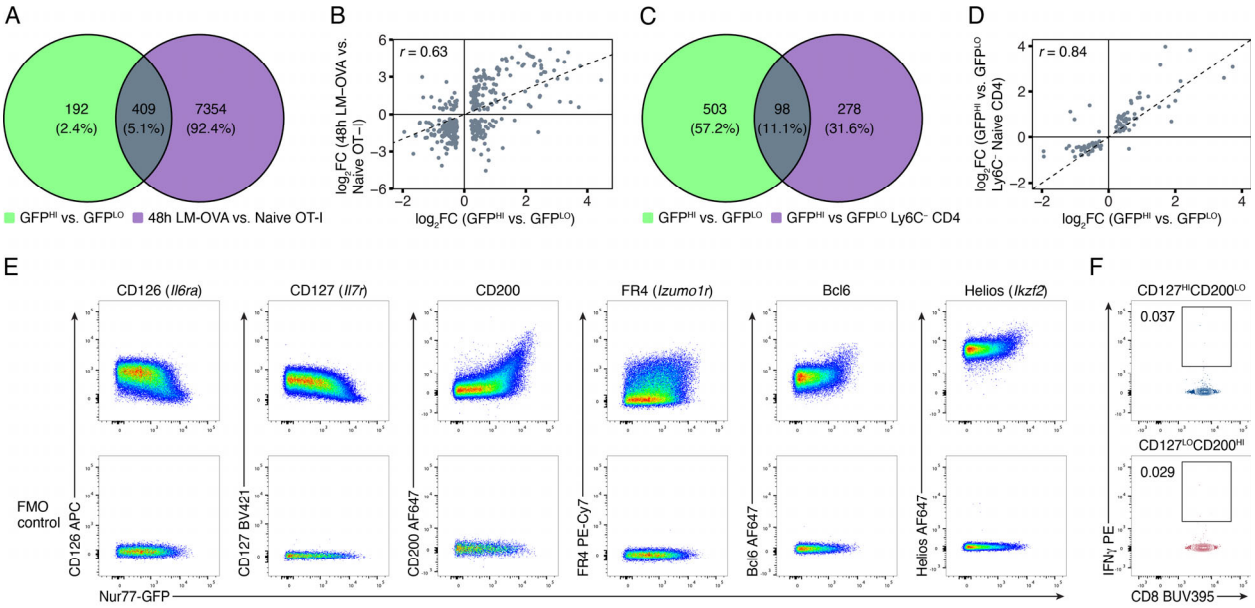

Fig. S5. Supporting data for the correlation between Nur77-GFP expression and differential gene expression in naive CD8$^+$ T cells. (**A**) Venn diagram of DEGs defined as genes with an FDR < 0.05 present in the GFP^{HI} versus GFP^{LO} naive OT-I dataset (green), the effector versus naive dataset (purple), or in both datasets (grey). The number of DEGs and the percentage of the total DEGs is depicted within each condition. (**B**) Log_2 fold-change plot of genes upregulated in effector compared to naive OT-I CD8$^+$ T cells on the Y-axis (*52*) and genes upregulated in GFP^{HI} compared to GFP^{LO} naive OT-I CD8$^+$ T cells on the X-axis. Each dot represents an overlapping DEG defined as in (A). The dotted black line depicts a 1:1 relationship between the two datasets. *r* indicates a Pearson's correlation coefficient, 95%CI= 0.57 to 0.69, $p < 0.0001$. (**C**) Venn diagram of DEGs defined as genes with an FDR < 0.05 present in the GFP^{HI} versus GFP^{LO} dataset (green), the GFP^{HI} versus GFP^{LO} CD4$^+$ Ly6C$^-$ dataset (purple) or in both datasets (grey). The number of DEGs and the percentage of the total DEGs is depicted within each condition. (**D**) Log_2 fold-change plot of genes upregulated in GFP^{HI} compared to GFP^{LO} naive Ly6C$^-$ CD4$^+$ T cells on the Y-axis (*7*) and genes upregulated in GFP^{HI} compared to GFP^{LO} naive OT-I CD8$^+$ T cells on the X-axis. *r* indicates a Pearson's correlation coefficient, 95%CI= 0.77 to 0.89, $p < 0.0001$. (**E**) The top row depicts Nur77-GFP expression in relationship to indicated markers in naive, polyclonal CD8$^+$ T cells. The bottom row indicates the fluorescence minus one (FMO) control for the indicated markers. Data represent two to three independent experiments from n = 3-6 mice. (**F**) Contour plots depict CD8 and IFNγ expression in unstimulated CD127^{HI} CD200^{LO} (top) and CD127^{LO} CD200^{HI} (bottom) polyclonal naive CD8$^+$ T cells after a 45 min IFNγ secretion assay. Data represent three independent experiments from n = 3 mice.

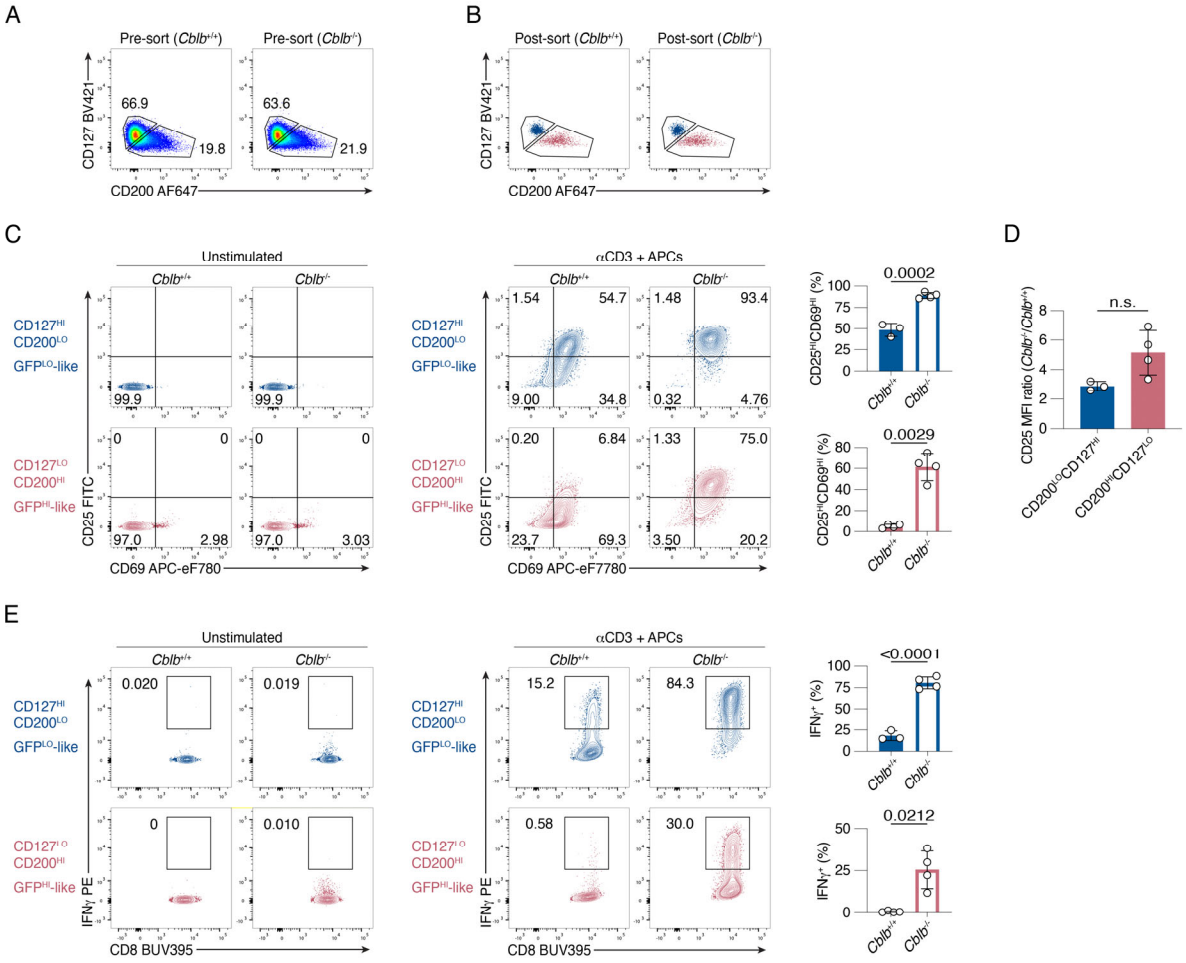

Fig. S6. Supporting data that increased Cbl-b expression in naive GFP^{HI} cells contributes to decreased responsiveness. (**A**) Dot plots depict the expression of CD127 and CD200 in naive, polyclonal CD8$^+$ T cells from *Cblb*$^{+/+}$ and *Cblb*$^{-/-}$ mice. (**B**) Representative flow cytometry plots of sorted, naive GFP^{LO}-like (blue) and GFP^{HI}-like cells (red) CD8$^+$ T cells from *Cblb*$^{+/+}$ and *Cblb*$^{-/-}$ mice. (**C**) Contour plots depict CD25 and CD69 expression in naive, polyclonal GFP^{LO} and GFP^{HI} CD8$^+$ T cells that were either unstimulated (left) or stimulated for 24 hours with 0.25 µg/ml anti-CD3 and APCs (right). Numbers indicate the percentage of cells within the indicated gates. Bar graphs show the percentages of CD25^{HI} CD69^{HI} cells. (**D**) Bar graph depicts the ratio of the CD25 MFI in *Cblb*$^{-/-}$ to *Cblb*$^{+/+}$ mice for CD200^{LO}CD127^{HI} (blue) and CD200^{HI}CD127^{LO} (red) cells. (**E**) Contour plots of IFNγ secretion from CD8$^+$ T cells that were either unstimulated (left) or stimulated as in C, after a 45-minute IFNγ secretion assay (right). Numbers indicate the percentage of cells within the indicated gates. Bar graphs show the percentages of IFNγ$^+$ cells. Bars (in C, D, and E) depict the mean, error bars depict ± s.d., and each symbol represents one biological replicate. Data in (A) to (E) represent three to four independent experiments with n = 3-4 biological replicates. Statistical testing was performed by unpaired two-tailed Student's t test in (C) (top) and (E) (top). Statistical testing was performed by unpaired two-tailed Student's t test with Welch's correction in (C) (bottom) and (E) (bottom), and D. n.s., not significant.

Table S1: Materials and reagents

REAGENT or RESOURCE	SOURCE	IDENTIFIER
Antibodies		
Anti-mouse CD3ε (Clone 145-2C11	BioLegend	Cat#100331; RRID:AB_1877073
Anti-mouse CD4, biotin (Clone RM4-5)	BioLegend	Cat#100508; RRID:AB_312711
Anti-mouse CD4, Pacific Blue (Clone RM4-5)	BioLegend	Cat#100531; RRID:AB_493374
Anti-mouse CD4, APC (Clone RM4-5)	BioLegend	Cat#100516; RRID:AB_312719
Anti-mouse CD5, BV786 (Clone 53-7.3)	BD Biosciences	Cat#740842; RRID:AB_2740496
Anti-mouse CD8a, biotin (Clone 53-6.7)	BioLegend	Cat#100704; RRID:AB_312743
Anti-mouse CD8a, PerCP-Cy5.5 (Clone 53-6.7)	BioLegend	Cat#100734; RRID:AB_2075238
Anti-mouse CD8a, PE-Cy7 (Clone 53-6.7)	BioLegend	Cat#100722; RRID:AB_312761
Anti-mouse CD8a, Pacific Blue (Clone 53-6.7)	BioLegend	Cat#100725; RRID:AB_493425
Anti-mouse CD8a, BV711 (Clone 53-6.7)	BioLegend	Cat#100759; RRID:AB_2563510
Anti-mouse CD8a, BV605 (Clone 53-6.7)	BioLegend	Cat#100744; RRID:AB_2562609
Anti-mouse CD8a, BUV395 (Clone 53-6.7)	BD Biosciences	Cat#563786; RRID:AB_2732919
Anti-mouse CD11b, biotin (Clone M1/70)	BioLegend	Cat# 101204; RRID:AB_312787
Anti-mouse CD11c, biotin (Clone N418)	BioLegend	Cat#117304; RRID:AB_313773
Anti-mouse CD16/CD32 (Fc Block) (Clone 2.4G2)	Tonbo Biosciences	Cat#70-0161-U500; N/A
Anti-mouse CD19, biotin (Clone 6D5)	BioLegend	Cat#115504; RRID:AB_313639
Anti-mouse CD19, Pacific Blue (Clone 6D5)	BioLegend	Cat#115523; RRID:AB_439718
Anti-mouse CD25, Pacific Blue (Clone PC61)	BioLegend	Cat#102022; RRID:AB_493643
Anti-mouse CD25, FITC (Clone PC61)	BioLegend	Cat#102006; RRID:AB_312855
Anti-mouse CD25, Al647 (Clone PC61)	BioLegend	Cat#102020; RRID:AB_493458
Anti-Mouse CD28 (Clone 37.51)	BioLegend	Cat#102112; RRID:AB_312877
Anti-mouse CD44, PE-Cy7 (Clone IM7)	BioLegend	Cat#103030; RRID:AB_830787
Anti-mouse CD44, PE (Clone IM7)	BioLegend	Cat#103008; RRID:AB_312959
Anti-mouse CD44, Pacific Blue (Clone IM7)	BioLegend	Cat#103020; RRID:AB_493683
Anti-mouse CD44, Al488 (Clone IM7)	BioLegend	Cat#103016; RRID:AB_493679
Anti-mouse CD44, Al647 (Clone IM7)	BioLegend	Cat#103018; RRID:AB_493681
Anti-mouse CD44, BUV496 (Clone IM7)	BD Biosciences	Cat#741057; RRID:AB_2870671
Anti-mouse CD44, BUV737 (Clone IM7)	BD Biosciences	Cat#612799; RRID:AB_2870126
Anti-mouse CD45.1, Pacific Blue (Clone A20)	BioLegend	Cat#110722; RRID:AB_492866
Anti-mouse CD45.2, PE-Cy7 (Clone 104)	BioLegend	Cat#109830; RRID:AB_1186098
Anti-mouse CD45.2, APC (Clone 104)	BioLegend	Cat#109814; RRID:AB_389211
Anti-mouse CD45R/B220, biotin (Clone RA3-6B2)	BioLegend	Cat#103204; RRID:AB_312989
Anti-mouse CD49b, biotin (Clone DX5)	BioLegend	Cat#108904; RRID:AB_313411
Anti-mouse CD62L, PE (Clone MEL-14)	BioLegend	Cat#104408; RRID:AB_313095
Anti-mouse CD62L, APC (Clone MEL-14)	BioLegend	Cat#104412; RRID:AB_313099
Anti-mouse CD62L, BUV737 (Clone MEL-14)	BD Biosciences	Cat#612833; RRID:AB_2870155
Anti-mouse CD69, PE-Cy7 (Clone H1.2F3)	eBioscience	Cat#25-0691-82; RRID:AB_469637
Anti-mouse CD69, eF780 (Clone H1.2F3)	eBioscience	Cat#47-0691-82; RRID:AB_2573966
Anti-mouse CD71, PE (Clone C2)	BD Biosciences	Cat#553267; RRID:AB_394744
Anti-mouse CD126, APC (Clone D7715A7)	BioLegend	Cat#115811; RRID:AB_2127937
Anti-mouse CD127, BV421 (Clone SB/199)	BD Biosciences	Cat#562959; RRID: AB_2737917
Anti-mouse CD200, Al647 (Clone OX-90)	BD Biosciences	Cat#565544; RRID:AB_2739287
Anti-mouse β2-microglobulin, PE (Clone A16041A)	BioLegend	Cat#154504; RRID:AB_2721340
Anti-mouse Bcl-6, Al647 (Clone K112-91)	BD Biosciences	Cat#561525; RRID:AB_10898007
Anti-Cbl-b (Clone D3C12)	Cell Signaling	Cat#9498; RRID:AB_2797707

Continued

REAGENT or RESOURCE	SOURCE	IDENTIFIER
Anti-mouse erythroid cells, biotin (Clone TER-119)	BioLegend	Cat#116204; RRID:AB_313705
Anti-mouse FR4, PE-Cy7 (Clone eBio12A5)	eBioscience	Cat#25-5445-80; RRID:AB_842812
Anti-mouse Helios, Al647 (Clone 22F6)	BD Biosciences	Cat#563951; RRID:AB_2738506
Anti-rabbit IgG AffiniPure Fab Fragment, APC	Jackson ImmunoResearch	Cat#711-136-152; RRID:AB_2340601
Anti-mouse IRF4, PE (Clone 3E4)	eBioscience	Cat#12-9858-80; RRID:AB_10853179
Anti-mouse TCRβ, APC (Clone H57-597)	BioLegend	Cat#109212; RRID:AB_313435
Anti-mouse TCRβ, BV711 (Clone H57-597)	BioLegend	Cat#109243; RRID:AB_2629564
Anti-mouse TCRβ, PE (Clone H57-597)	BD Biosciences	Cat#553172; RRID:AB_394684
Anti-mouse TCR Vα2, PE (Clone B20.1)	BioLegend	Cat#127808; RRID:AB_1134183
Anti-mouse TCR Vα2, BV605 (Clone B20.1)	BD Biosciences	Cat#747768; RRID:AB_2872232
Anti-mouse Qa-2, biotin (Clone 695H1-9-9)	BioLegend	Cat#121703; RRID:AB_572000
Virus strains		
LCMV Armstrong	Dr. Rafi Ahmed (Ahmed *et al*., 1984) (*109*)	N/A
Chemicals and peptides		
OVA (257-264) (SIINFEKL)	GenScript	Cat#RP10611
OVA (257-264) (SIIQFERL)	GenScript	Custom
OVA (257-264) (SIIGFEKL)	GenScript	Custom
OVA (257-264) (SIIVFEKL)	In house (University of Utah)	N/A
GP33-41 (KAVYNFATC)	GenScript	Cat#RP20091
LIVE/DEAD Fixable Near-IR	Thermo Fisher Scientific	Cat#L34976
LIVE/DEAD Fixable Violet	Thermo Fisher Scientific	Cat#L34955
LIVE/DEAD Fixable Yellow	Thermo Fisher Scientific	Cat#L34967
Ghost Dye Red 780	Cytek Biosciences	Cat#13-0865-T100
CellTrace Violet	Thermo Fisher Scientific	Cat#C34557
Indo-1 AM	Thermo Fisher Scientific	Cat#I1223
Streptavidin (APC)	Thermo Fisher Scientific	Cat#SA1005
Streptavidin (eFluor 450)	eBioscience	Cat#48-4317-82
BD Perm/Wash buffer	BD Biosciences	Cat#554723
Foxp3 Staining buffer set	eBioscience	Cat#00-5523-00
RBC lysis buffer	Tonbo Biosciences	Cat#TNB-4300-L100
RPMI 1640	Thermo Fisher Scientific	Cat#11875-119
Fetal bovine serum	Omega Scientific	Cat#FB-21
HEPES	Thermo Fisher Scientific	Cat#15630-080
MEM non-essential amino acid solution	Sigma-Aldrich	Cat#M7145-100ML
Penicillin-streptomycin-glutamine	Thermo Fisher Scientific	Cat#10378-016
Sodium pyruvate	Sigma-Aldrich	Cat#S8636-100ML
2-Mercaptoethanol	Thermo Fisher Scientific	Cat#31350-010
Critical commercial assays		
Mouse IFN-γ Secretion Assay – Detection Kit (PE)	Miltenyi Biotec	Cat#130-090-516
Mouse IFN-γ Secretion Assay – Detection Kit (APC)	Miltenyi Biotec	Cat#130-090-984
Mouse IL-2 Secretion Assay – Detection Kit (APC)	Miltenyi Biotec	Cat#130-090-987
EasySep Mouse Streptavidin RapidSpheres Isolation Kit	STEMCELL Technologies	Cat#19860A
Deposited data		
RNA-seq (raw data and count data)	This study	GEO: GSE223457

Continued

REAGENT or RESOURCE	SOURCE	IDENTIFIER
Experimental models: Organisms/strains		
C57BL/6J	Jackson Laboratory	Cat#000664; RRID:IMSR_JAX:000664
B6.SJL-Ptprca Pepcb/BoyJ	Jackson Laboratory	Cat#002014; RRID:IMSR_JAX:002014
B6.129P2-B2mtm1Unc/DcrJ	Jackson Laboratory	Cat#002087; RRID:IMSR_JAX:002087
Zap70tm1Weis	Kadlecek *et al.*, 1998 (*91*)	N/A
Tg(Nr4a1-EGFP)GY139Gsat	Zikherman *et al.*, 2013 (*14*)	N/A
Nur77-GFP-Foxp3-RFP	Zinzow-Kramer *et al.*, 2019 (*18*)	N/A
OT-I-Nur77-GFP-*Trca*$^{-/-}$	This study	N/A
P14-Nur77-GFP	This study	N/A
Cbl-b$^{-/-}$	Chiang *et al.*, 2000 (*95*)	N/A
Nur77-GFP-***Cbl-b***$^{-/-}$	This study	N/A
Oligonucleotides		
Atto647N-biotin labeled ligand strand: **Atto647N** - CGC ATC TGT GCG GTA TTT CAC TTT - **Biotin**	Ma *et al.*, 2019 (*48*)	N/A
DBCO-BHQ2 labeled quencher strand: **DBCO** - TTT GCT GGG CTA CGT GGC GCT CTT - **BHQ2**	Ma *et al.*, 2019 (*48*)	N/A
Hairpin strand: GTG AAA TAC CGC ACA GAT GCG TTT GTA TAA ATG TTT TTT TCA TTT ATA CTTTAA GAG CGC CAC GTA GCC CAG C	Ma *et al.*, 2019 (*48*)	N/A
Software and algorithms		
FlowJo V10	BD Biosciences	https://www.flowjo.com
Gene Set Enrichment Analysis (GSEA)	Subramanian *et al.*, 2005 (*105*)	https://www.gsea-msigdb.org/gsea
Prism 9	GraphPad Software	https://www.graphpad.com
R (version 4.1.1) and dependencies	The Comprehensive R Archive Network	https://cran.r-project.org/
Other		
BD Quantibrite PE beads	BD Biosciences	Cat#340495